

Original Article

Advantages of contrast-enhanced CT combined with DCE-MRI in identifying malignant parotid tumor

Dongping Deng, Hongfeng Dong

Department of Radiology, The First People's Hospital of Huzhou, Huzhou, Zhejiang, China

Received September 11, 2022; Accepted November 14, 2022; Epub December 15, 2022; Published December 30, 2022

Abstract: Objective: To study the value of single and combined application of contrast-enhanced computerized tomography (CT) and dynamic contrast enhanced magnetic resonance imaging (DCE-MRI) in diagnosing parotid tumors. Methods: In this retrospective study, 82 patients with parotid gland mass who received contrast-enhanced CT and DCE-MRI detection in The First People's Hospital of Huzhou from March 2018 to March 2022 were selected as study subjects. The nature of the parotid tumor was pathologically examined following the surgery. According to the pathological diagnosis results, these patients were divided into a benign group (n=59) and a malignant group (n=23). All patients underwent contrast-enhanced CT and DCE-MRI examinations. The diagnostic accuracy rates of contrast-enhanced CT, DCE-MRI and the joint application were compared. The CT or MRI images of benign and malignant parotid tumors were compared. The correlation of parotid cancer with the imaging features was analyzed. Diagnostic efficiency of contrast-enhanced CT, DCE-MRI and joint application for parotid cancer was assessed by receiver operating characteristic curve. Results: In terms of diagnostic accuracy, there was a significant difference between contrast-enhanced CT combined with DCE-MRI and contrast-enhanced CT alone (95.12% vs. 81.71%, $P<0.001$), and between the joint application and DCE-MRI alone (95.12% vs. 86.58%, $P=0.004$). Results of contrast-enhanced CT revealed statistical differences in tumor boundary, tumor size, calcification and cystic degeneration between benign and malignant tumors ($P<0.05$), but no obvious difference in lymph node enlargement between the two groups. MRI results showed that there were differences in the DCE-MRI time-signal intensity curve and ADC value between benign and malignant tumors ($P<0.05$). Correlation analysis results showed that the malignant tumor was negatively correlated with tumor boundary, calcification, cystic degeneration and ADC values, and it was positively correlated with DCE-MRI time-signal intensity curve and tumor size ($P<0.05$). Analysis of diagnostic efficacy showed that contrast-enhanced CT combined with DCE-MRI were significantly better than contrast-enhanced CT alone in terms of sensitivity and specificity ($P<0.05$). Moreover, the sensitivity of the joint application was also higher than that of MRI alone, while no obvious difference was found for specificity between joint application and MRI alone. The areas under the curve of contrast-enhanced CT combined with DCE-MRI in diagnosing malignant parotid tumor was remarkably greater than that of CT or MRI alone ($P<0.05$). Conclusion: Contrast-enhanced CT combined with DCE-MRI can significantly improve the diagnostic accuracy, sensitivity and specificity for malignant parotid tumor, and the joint application was able to point out the direction of targeted surgical treatment plans.

Keywords: Parotid tumors, CT, MRI, diagnosis, clinical value

Introduction

The parotid gland is located in the superficial tissue of the external auditory canal located inferior and anteriorly in the human face and it is considered to be the largest gland within the human salivary glands. Among all head and neck tumors, the incidence of parotid tumors is approximately 5%, and it mainly occurs in populations with an age ranging from 30 to 50 years old [1]. When parotid tumors occur, obvious

masses and swelling can be seen on the face. Clinically parotid tumors are mostly benign, accounting for about 80% of all patients with parotid tumors [2]. Such patients usually have a better prognosis after surgical treatment, but there are still about 20% of patients with parotid malignancy, among whom the disease relapses after surgical treatment [3]. At present, the pathogenesis of parotid tumors has not been clarified, and it has been reported that its inducements were related to smoking, oral

Identification of parotid tumors by CT plus MRI

hygiene, local irritation and so on [4]. Due to the complex and diverse pathological types of parotid tumors, the lack of specific tumor markers, and the insignificant clinical symptoms, there are certain errors in the clinical differential diagnosis between benign and malignant parotid tumors [5, 6]. In patients with early parotid tumors, there are no obvious clinical manifestations except for a significant mass in the parotid area. As the disease progresses, if it deteriorates into a malignant tumor, it may metastasize to other adjacent tissues and cause corresponding symptoms. Effective identification of benign and malignant lesions in patients with parotid tumors at the early stage is of great significance for guiding treatments and improving prognosis [7]. Although pathological biopsy can confirm the diagnosis, it is not recommended to perform local fine-needle aspiration biopsy before surgery. First of all, most of the tumors are in special locations. Fine-needle aspiration biopsy would cause sampling errors, resulting in reduced sensitivity and specificity. Secondly, fine-needle aspiration biopsy may lead to the metastasis of malignant tumors and the infection of some benign tumors [8, 9]. Therefore, at present, the preoperative diagnosis of parotid tumors is still dominated by imaging technology, and it is very important to reduce the errors by improving the performance of imaging diagnosis.

In clinical practices, non-invasive examination methods for parotid tumors include ultrasound, magnetic resonance imaging (MRI) and computed tomography (CT). The use of ultrasound in parotid gland tumors has certain limitations, because ultrasound is regarded to be more suitable for detecting superficial glands. When the tumor is located in the deep lobes of parotid gland or in the minor salivary glands, it is difficult for the ultrasound to clearly display the images [10]. CT can accurately locate the mass of the parotid gland, and clearly show the size, number, shape, boundary and infiltration of the surrounding tissues. It was reported that contrast-enhanced CT could clearly display the retromandibular vein, carotid artery and structures of cervical lymph node, which provided evidence for surgical treatment [11]. Some studies reported that CT could make an accurate qualitative diagnosis of typical benign and malignant parotid tumors, but it has certain limitations for the diagnosis of low-grade malig-

nant tumors [12, 13]. Another study also reported that CT was of great significance for the diagnosis in the morphological aspects such as tumor lesion boundary definition, tumor size, calcification and cystic degeneration, but there were shortcomings such as insufficient diagnostic accuracy [14]. MRI is currently another examination for the identification of parotid gland tumors. However, using MRI examination alone has some limitations. It was reported that MRI examination was not able to obtain the internal microstructure of tumor tissues, resulting in difficulty in evaluating the risk of parotid tumors [15]. Some studies have shown that diffusion-weighted MRI could well reveal the tissue of the tumor with abundant vascularity, but the diagnostic value for malignant parotid tumors is debated [16]. Another study showed that MRI could improve the diagnostic accuracy by analyzing the local blood flow in the soft tissue, but it has limitations in terms of morphology [17]. So far, only a limited amount of data are found regarding the value of CT combined with MRI for the differential diagnosis between benign and malignant parotid tumors. In this context, this research included 82 cases of parotid tumors to investigate the roles of CT plus MRI for identifying parotid tumors, so as to provide evidence for identifying the nature of parotid tumors.

Material and methods

General information

In this retrospective study, 82 patients with parotid gland mass admitted from March 2018 and March 2022 were selected as the research subjects. Inclusion criteria: (1) patients over 18 years old who were diagnosed with parotid gland mass according to the criteria [2]; (2) patients with only a solitary lesion; (3) patients with no history of endocrine treatment, radiotherapy or chemotherapy; (4) patients who voluntarily received contrast-enhanced CT and MRI; (5) patients who received fine-needle aspiration biopsies or surgical resection, and the tumorous nature was verified by the histopathological examination; (6) patients with complete medical records. Exclusion criteria: (1) patients with a history of other malignant tumors; (2) patients with a history of parotid gland surgery; (3) patients with a hypersensitivity reaction of the contrast agent; (4) patients

Identification of parotid tumors by CT plus MRI

with contraindications of MRI such as metal implants in the body; (5) patients with severe renal or hepatic dysfunctions, cardio-and cerebrovascular diseases or mental disorder. All the patients were informed about the necessity for pathological detection and about the examination of contrast-enhanced CT and MRI performed prior to the biopsy. According to the pathological diagnosis, these patients were divided into a benign group and a malignant group. The Ethics Committee of The First People's Hospital of Huzhou approved this research (No. 2018-014).

Methods

CT was conducted using Siemens Definition AS 64-row 128-layer spiral CT. Patients were maintained in the supine position, and the scanning scope included the parotid region and neck. The parameters were as follows: the 0.8 pitch, 3 mm section gap, 3 mm section gap, 125 kV and 250 mA. Contrast-enhanced CT was conducted following intravenous injection of Ioversol (350 mgI/mL) at the speed of 3.0 mL/s via a double-syringe power injector. After the scan, the obtained images were transmitted to the workstation, and then the imaging features including location of lesions, shape, density, margin, cystic necrosis, degree of enhancement, invasion of adjacent structures and lymphadenopathy were analyzed by radiologists.

MRI examination was performed using 1.5T Philips Ingenia magnetic resonance scanner. Patients were kept in a supine position and the scanning scope involved the entire parotid gland. Routine plain scan was conducted according to the following arguments: fast spin echo (FSE) sequence sagittal T1-weighted image (T1WI), T2-weighted image (T2WI), transverse axis [time of echo (TE) 127 ms, time of repetition (TR) 3970 ms], matrix 256 × 87; sagittal fat-saturated T2-weighted image (TE 84 ms, TR 4000 ms); spin echo (SE) sequence sagittal T1WI and T2WI, transverse axis (TE 19 ms, TR 412 ms), matrix 256 × 75. The obtained imaging data were analyzed after scanning. Dynamic contrast enhanced magnetic resonance imaging (DCE-MRI) was performed using fat suppression three-dimensional disturbing gradient echo (T1-FFE) sequence with 15 mL of contrast agent (Gadoterate meglumine, specifi-

cation: 15 ml:5.654 g) plus 20 mL of normal saline, which were injected via the double-syringe power injector (speed 2.0 mL/s). After 3 scans, the obtained data were plotted as a time-signal intensity curve. The spin-echo echo planar imaging (SE-EPI) sequence scan was also performed, and the apparent diffusion coefficient (ADC) values were recorded.

According to the morphological manifestations, the edges of the enhanced lesions were divided into smooth, irregular and speculation. The enhancement appearances were divided into even, uneven and annular enhancement. The functool software was used to select a region of interest in the largest and most significant enhancement lesion, trying to avoid blood vessels, necrosis and cystic degeneration areas that can be distinguished by the naked eye and identifying the area that was slightly smaller than the lesion range (<10 mm²). The time-signal intensity curve was obtained and divided into three types [18]. Type I: the curve was slowly and continuously rising (the signal intensity elevated >10% between 3-8 time phase); type II: obvious enhancement appeared in the early stage, and the plateau level was maintained in the middle and late stages (the signal intensity increased or decreased within ±10% between 3-8 time phase); type III: obvious enhancement appeared in the early stage, and the signal intensity remarkably decreased by 10% in the middle and late stages between 3-8 time phase.

The analysis of data regarding contrast-enhanced CT and DCE-MRI was performed by two experienced radiologists with more than 10 years of work experience. The diagnostic criteria of CT and MRI were conducted according to previous studies [15, 19-21]. When there was a disagreement in the results, it was determined after joint discussion.

Statistical methods

Using pathological results as the gold standard, the diagnostic value including sensitivity, specificity and accuracy of contrast-enhanced-CT, DCE-MRI and the combined application for parotid cancer was analyzed. Diagnostic efficiency of contrast-enhanced-CT, DCE-MRI and the combined application was also assessed via receiver operating characteristic (ROC). All the clinical data obtained in the research were

Identification of parotid tumors by CT plus MRI

Table 1. The comparison of basic data between benign and malignant groups

Parameters	Benign group (n=59)	Malignant group (n=23)	t/ χ^2 value	P value
Age (years)	50.6±5.1	52.7±5.2	1.616	0.110
Male/Female	29/30	11/12	0.012	0.914
Location			4.411	0.220
Left superficial lobe	17	6		
Left deep lobe	14	5		
Right deep lobe	9	8		
Right superficial lobe	19	4		
Course of disease (years)	1.86±0.52	1.92±0.54	0.464	0.644

analyzed using SPSS 26.0. The measurement data were described in the form of mean \pm standard deviation, and the comparison was conducted by t test. The count data were showed in the form of percentages/cases, and the comparison among groups was conducted using χ^2 test. The correlation between malignant tumors and imaging signs was analyzed by Spearman correlation analysis. $P < 0.05$ indicated a significantly statistical difference.

Results

Basic data

As described in **Table 1**, there were 59 patients with benign parotid tumor and 23 patients with malignant parotid tumor included in this research. There was no statistical difference in the age, sex, location of disease and course of disease between benign and malignant groups (all $P > 0.05$). So, the two groups were comparable. The images of CT or MRI examinations were shown in **Figure 1**.

Comparison of diagnostic accuracy rate

The included 82 patients with parotid tumors were pathologically diagnosed, and there were 42 patients with pleomorphic adenoma, 13 patients with adenolymphoma and 4 patients with hemangioma in benign group, while in the malignant group, there were 12 cases with mucoepidermoid carcinoma, 6 cases with adenocystic cancer and 5 cases with parotid metastases. The diagnostic accuracy rate of CT combined with MRI was 95.12%, which was significantly higher than that of CT alone (81.71%) or MRI alone (86.58%), as shown in **Table 2**. Moreover, among them, the diagnostic accu-

rate of metastatic parotid tumors was the lowest in these three diagnostic methods.

Comparison of imaging features of contrast-enhanced CT between benign and malignant parotid tumors

The included 82 patients with parotid tumors underwent contrast-enhanced CT, and the results were shown in **Table 3**. In the benign group, there were 54 patients with clear boundary and

5 patients with obscure boundary. The average size of the tumor was $8.22 \pm 1.34 \text{ cm}^3$. There were 22 cases with calcification and cystic degeneration, and 37 cases without. There were 12 patients with lymph node enlargement and 47 patients without. In the malignant group, there were 9 patients with clear boundary and 14 patients with obscure boundary. The average size of the tumor was $14.25 \pm 1.65 \text{ cm}^3$. All patients were without calcification and cystic degeneration. There were 6 patients with lymph node enlargement and 17 patients without. Statistical differences were observed in term of tumor boundary, tumor size, calcification and cystic degeneration between the two groups ($P < 0.001$), while there was no obvious difference in lymph node enlargement between the two groups.

Comparison of imaging features of DCE-MRI between benign and malignant parotid tumors

The included 82 patients with parotid tumors received DCE-MRI, and the results were shown in **Table 4**. In the benign group, there were 29 patients with type I, 24 patients with type II and 6 patients with type III, and the value of ADC was 1.72 ± 0.22 . While in the malignant group, there were 3 cases with type I, 3 cases with type II and 17 cases with type III, and the value of ADC was 1.01 ± 0.14 . Obvious differences were found in time-signal intensity curve and ADC values between the two groups.

Correlation analysis between malignant parotid tumors and imaging features

The results of correlation analysis between malignant parotid tumors and imaging features were shown as follows: clear boundary: -0.623,

Identification of parotid tumors by CT plus MRI

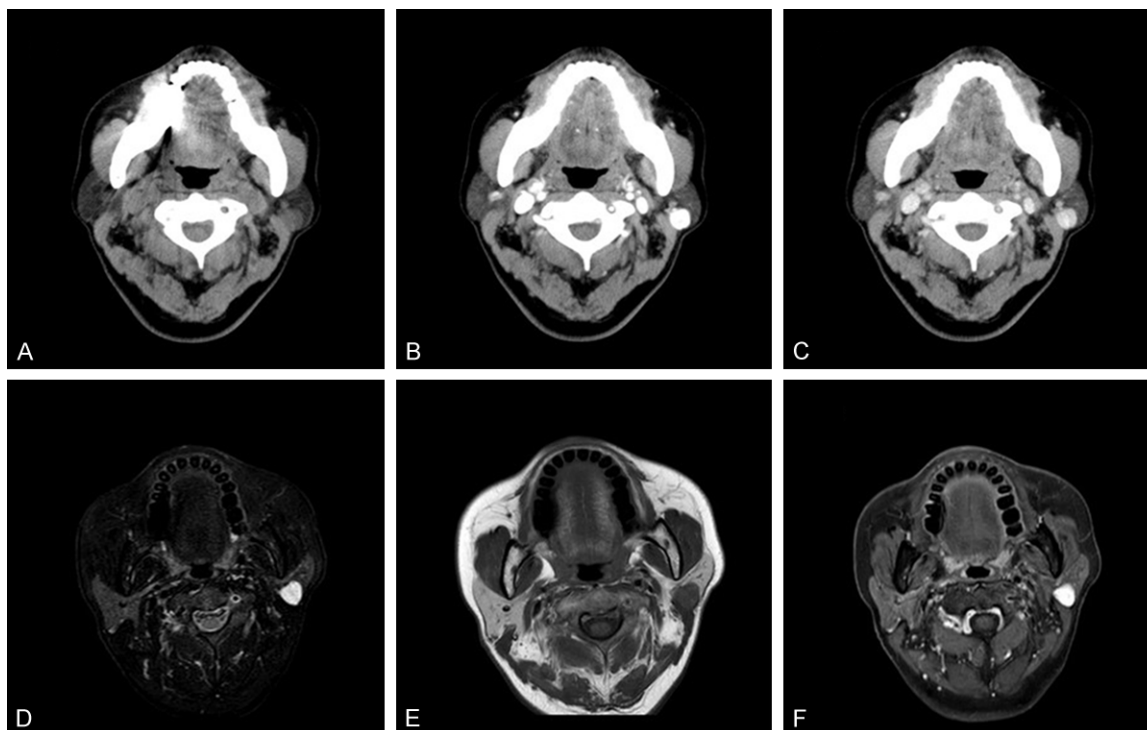


Figure 1. The images of computerized tomography (CT) and magnetic resonance imaging (MRI) in patients with left parotid hemangioma before surgery. A: CT scan showed a round, slightly low-density mass in the left parotid gland, with clear boundary and homogenous density. The size of tumor was about 13 × 12 mm. B: Contrast-enhanced CT in arterial phase showed obvious homogenous enhancement in the arterial phase after enhancement. C: Contrast-enhanced CT in venous phase showed continuous enhancement in the venous phase, and the density was similar to that of the large blood vessels in the same layer. There were no obvious enlarged lymph nodes in the neck region. D: T2WI mDixon technique showed a superficial lobulated mass in the left parotid gland. The mass was obviously present in high signal, homogenous signal and clear boundary. The size of tumor was about 14 × 11 mm. E: T1WI Scan showed that the left parotid gland tumor was iso- or hypo-intense signal, with obvious enhancement on contrast enhanced CT scan, and the boundary was clear. F: T1WI mDixon showed that the left parotid gland lesion had significantly homogeneous density, with clear boundary, and no obvious enlarged lymph node was found in the neck region.

Table 2. Comparison of diagnostic accuracy of parotid tumors among CT alone, MRI alone and the combined application [Case (%)]

Tumor types	Pathological diagnosis (Cases)	Contrast-enhanced CT	DCE-MRI	The combined application
Pleomorphic adenoma	42	37 (88.09)	39 (92.85)	41 (97.62)
Adenolymphoma	13	10 (76.92)	11 (84.62)	12 (92.31)
Angioma	4	3 (75.00)	3 (75.00)	4 (100)
Mucoepidermoid carcinoma	12	9 (75.00)	10 (83.33)	11 (91.67)
Adenoid cystic carcinoma	6	5 (83.33)	5 (83.33)	6 (100)
Parotid gland metastatic tumor	5	3 (60.00)	3 (60.00)	4 (60.00)
Total	82	67 (81.71)	71 (86.58)	78 (95.12)

P=0.004; calcification and cystic degeneration: -0.524, P=0.001; ADC: -0.385, P=0.005; tumor size: 0.280, P=0.012; time-signal intensity curve: 0.249, P=0.024. Obvious statistical differences were obtained in the correlation of

malignant parotid tumors with clear boundary, calcification and cystic degeneration, tumor size and time-signal intensity curve. Malignant parotid tumor was negatively associated with clear boundary, calcification and cystic degen-

Identification of parotid tumors by CT plus MRI

Table 3. Comparison of imaging features of contrast-enhanced computerized tomography (CT) between benign and malignant groups

Parameters	Benign group	Malignant group	χ^2 value	P value
Tumor boundary (Cases)			18.325	<0.001
Clearness	54	9		
Obscureness	5	14		
Tumor size (cm ³)	8.22±1.34	14.25±1.65	16.953	<0.001
Calcification and cystic degeneration (Cases)			10.724	0.001
Yes	22	0		
No	37	23		
Lymph node enlargement (Cases)			0.856	0.442
Yes	12	6		
No	47	17		

Table 4. Comparison of imaging features of dynamic contrast enhanced magnetic resonance imaging (DCE-MRI) between benign and malignant groups

Groups	Time-signal intensity curve (Cases)			ADC value
	Type I	Type II	Type III	
Benign group	29	24	6	1.72±0.22
Malignant group	3	3	17	1.01±0.14
χ^2		32.195		15.168
P		<0.001		<0.001

eration and ADC values, while it was positively associated with tumor size and time-signal intensity curve, and the coefficient of association was 0.280 and 0.249.

Diagnostic efficiency of contrast-enhanced CT alone, DCE-MRI alone and the combined application

The diagnostic efficiency of these methods was shown in **Table 5**. The sensitivity of the combined application was 94.74%, which was obviously higher than that of contrast-enhanced CT alone (70.96%, $P<0.001$) or DCE-MRI alone (86.21%, $P=0.012$). In addition, the specificity of contrast-enhanced CT alone, DCE-MRI alone and combined application was 37.25%, 39.62% and 40.91%, respectively. Obvious differences were observed for specificity between contrast-enhanced CT alone and the combined application ($P=0.034$). There was no statistical difference in specificity between DCE-MRI alone and the combined application.

Comparison of ROC results

The area under curve (AUC) of contrast-enhanced CT, MRI and the combination for

parotid gland cancer was 0.578, 0.648 and 0.791, respectively. The AUC of the combination for diagnosing parotid cancer was remarkably higher than that of CT or MRI alone ($P=0.016$). See **Table 6** and **Figure 2**.

Discussion

The parotid gland is considered as the largest pair of salivary glands in the body [22]. As the most common tumor of the neck seen in clinical practice, the diagnosis of parotid tumors still needs to be confirmed by pathological biopsy, and surgery is still the first choice for treatment [23]. Among them, local parotidectomy is mainly used for benign parotid tumors, and total parotidectomy is used for malignant parotid tumors. It can be seen that the type of tumor needs to be clearly defined before surgery. The choice of surgical approach is very important [24-26]. Some studies have shown that pathological biopsy, CT and MRI have their own unique advantages in distinguishing benign and malignant parotid tumors [27]. Among them, the accuracy rate of pathological biopsy is as high as 98%, which is an important method of diagnosis. However, many studies revealed that the incidence of complications such as bleeding and pain discourage a large number of patients from agreeing to be involved in the needle biopsy operation. Thus, the optimal detective technology for malignant parotid tumor is non-invasive, with less damage, less side effects and still of benefit to a high proportion of patients. CT can display the tumor morphology more clearly, and MRI has advantages in the analysis of blood flow signals, which can significantly improve the

Identification of parotid tumors by CT plus MRI

Table 5. Comparison of diagnostic efficiency among computerized tomography (CT) alone, magnetic resonance imaging (MRI) alone and the combined application

Diagnostic methods	True positives (Cases)	False positive (Cases)	True negatives (Cases)	False negatives (Cases)	Sensitivity [% (n/m)]	Specificity [% (n/m)]
CT	22	32	19	9	70.96 (22/31)	37.25 (19/51)
MRI	25	40	13	4	86.21 (25/29)	39.62 (13/53)
CT combined with MRI	36	26	18	2	94.74 (36/38)	40.91 (18/44)

Table 6. Comparison of ROC results of CT, MRI and the combined application for parotid cancer

Groups	AUC	SE	95% CI
CT	0.578	0.050	0.497~0.785
MRI	0.648	0.039	0.462~0.819
CT plus MRI	0.791	0.043	0.667~0.903

diagnostic accuracy, sensitivity and specificity non-invasively. In this study, CT combined with MRI was used to comprehensively evaluate the changes in morphology and blood flow signals so as to diagnose benign and malignant parotid tumors, and the performance of the imaging examinations was evaluated.

There is limited data regarding the diagnostic efficacy of CT combined with MRI in malignant parotid tumors. Using the features of CT and MRI, the strong points of both were achieved by combined application. It was previously reported that in CT images, pleomorphic adenomas showed round or oval soft tissue mass; adenolymphomas showed round cystic mass, hemangiomas showed characteristically popcorn-shaped changes; mucoepidermoid carcinoma showed irregular in contour of tumors; adenoid cystic carcinomas could invade the surrounding structures and display a regular or irregular boundary; parotid gland metastases lacked smooth in boundary and are located in the deep lobes [11]. Therefore, contrast-enhanced CT has certain advantages in judging the histomorphology of tumors and can quickly perform differential diagnosis between benign and malignant parotid tumors through morphological analysis [28]. In this study, benign parotid tumors had continuous and well-defined boundary, while malignant parotid tumors had obscure boundary, which is consistent with the above study. However, studies have also reported that although CT can quickly conduct differential diagnosis between benign and malignant

parotid tumors, the diagnostic accuracy and specificity were inadequate, and radiation risk and contrast agent tolerance were the limitations of CT [29].

MRI was helpful to accurately identify the position of different tumors through the analysis of blood flow signals, including tumor size, location, nature, invasion and lymph node metastasis, which is more convincing than the morphological observation of CT images [30]. For example, T1 and T2 weighted images could clearly display the texture of malignant parotid tumor, including the areas of normal and diseased tissues. It was reported that malignant parotid tumors could be distinguished through obscure boundary, cystic components, low T2 signal intensity, necrosis and infiltration to adjacent tissues in conventional MRI images [31]. In this study, the results of the DCE-MRI time-signal intensity curve showed that benign tumors were mainly type I and II, while malignant tumors were mostly type III. It was indicated that it was not possible to evaluate only the shape and size of tumor in the clinical diagnosis of benign and malignant parotid tumors. The results of this study suggested that there was a close correlation of malignant tumors with boundary definition, calcification and cystic degeneration rates, ADC, and DCE-MRI time-signal intensity curves. Our analysis showed that in the progression of malignant tumors, the malformations rate of vascularization caused by the compression of local tissues was obviously increased, because tumor cells need to absorb more nutrients in the process of proliferation. The following inflammation would further aggravate the deterioration of tumor.

Some studies have showed that the ADC value can reflect the degree of angiogenesis under the condition of eliminating blood perfusion interference [32]. In this study, it was found that the ADC value in the benign group was

Identification of parotid tumors by CT plus MRI

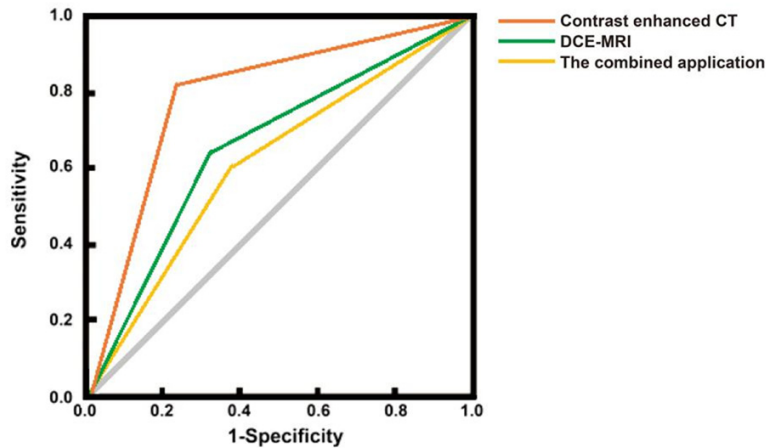


Figure 2. ROC curve of different examination methods for diagnosing malignant parotid tumors.

1.72±0.22, which was significantly higher than that in the malignant group (1.01±0.14). The possible reasons were as follows: the nuclei of malignant tumor cells were significantly larger than those of benign tumor cells, and the shape of malignant tumor cells was irregular, so the increasing growth rate was faster and the growth pattern was also irregular, thereby the local water diffusion capacity in the lesion was reduced. All of these resulted in an increase in the degree of neovascular malformations, and the reduction of local elasticity of the deformed blood vessels which could lead to an increase in blood flow resistance, ultimately decreasing the ADC value. Previous studies have showed that there was a certain correlation between ADC values and the deterioration of tumors, which is similar to the results of this study [33]. It was more convincing to judge the invasive ability of tumors by analyzing the metabolic capacity of the local tissue in tumor by the conditions of blood perfusion (ADC value). However, the disadvantage was that the morphological analysis could not be well performed by using MRI alone. Therefore, there were certain limitations of MRI or CT alone for patients with parotid tumors. In addition, the AUC of combined application was obviously more than that of CT or MRI alone, with remarkable statistical differences. It was indicated that CT combined with MRI had significant advantages in the term of diagnosing parotid malignant tumors, which is in accordance with previous reports [34].

The current study has some shortcomings that should be recognized. First, this is a retrospective study, which could not conduct blind analy-

sis, randomization and power calculation. Second, the sample size in this study was small, which may affect the findings. Third, the clinical data regarding patients were obtained from a single center, which might affect its generalization to other hospitals. In future studies, it is required to confirm our findings by increasing the sample size and adopting multi-center and randomized prospective studies.

In conclusions, although CT or MRI revealed relatively high sensitivity and specificity in detecting malignant parotid tumors, the combination of the two yields a higher diagnostic efficacy. A satisfactory finding of combined application seems to be achieved by analysis of morphology and blood flow signal. So, this combination has the potential to play an important role in the diagnosis and prognosis assessment of malignant parotid tumors, and must be further investigated.

Disclosure of conflict of interest

None.

Address correspondence to: Hongfeng Dong, Department of Radiology, The First People's Hospital of Huzhou, No. 158 Guangchanghou Road, Huzhou 313000, Zhejiang, China. Tel: +86-0572-2051000; Fax: +86-0572-2051000; E-mail: donghongfeng_hz@163.com

References

- [1] Welkoborsky HJ, Albers M and Kustermeyer J. Perfusion analysis of benign parotid gland tumors by contrast-enhanced ultrasonography (CEUS). *Eur Arch Otorhinolaryngol* 2022; 279: 4137-4146.
- [2] Maahs GS, Oppermann Pde O, Maahs LG, Machado Filho G and Ronchi AD. Parotid gland tumors: a retrospective study of 154 patients. *Braz J Otorhinolaryngol* 2015; 81: 301-306.
- [3] Gerwel A, Kosik K and Jurkiewicz D. US in pre-operative evaluation of parotid gland neoplasms. *Otolaryngol Pol* 2015; 69: 27-33.
- [4] Grasso M, Fusconi M, Cialente F, de Soccio G, Ralli M, Minni A, Agolli G, de Vincentiis M, Remacle M, Petrone P, Di Maria D, D'Andrea V

Identification of parotid tumors by CT plus MRI

- and Greco A. Rupture of the pleomorphic adenoma of the parotid gland: what to know before, during and after surgery. *J Clin Med* 2021; 10: 5368.
- [5] Matsumoto F, Ohba S, Fujimaki M, Kojima T, Sakyo A, Kojima M and Ikeda K. Efficacy of modified face lift incision for the resection of benign parotid gland tumor located anteriorly or superiorly. *Auris Nasus Larynx* 2021; 48: 978-982.
- [6] Ning Y, Wang W, Cai Y, Zhou Y, Jiang J, Zeng D, Sun R, Wang X, Zheng W, He T, Shui C, Liu W, Zhang Y, Chen X and Li C. The application of venous nerve conduit trap in the immediate repair and reconstruction of facial nerve in parotid gland tumor: an attempt of a new technique. *Eur Arch Otorhinolaryngol* 2021; 278: 4967-4976.
- [7] Park YM and Koh YW. Current issues in treatment of parotid gland cancer and advanced surgical technique of robotic parotidectomy. *Curr Oncol Rep* 2022; 24: 203-208.
- [8] Baba A, Kessoku H, Akutsu T, Shimura E, Matsushima S, Kurokawa R, Ota Y, Suzuki T, Kawasumi Y, Yamauchi H, Ikeda K and Ojiri H. Pre-treatment MRI predictor of high-grade malignant parotid gland cancer. *Oral Radiol* 2021; 37: 611-616.
- [9] Mantsopoulos K, Sievert M, Iro AK, Muller SK, Koch M, Schapher M, Agaimy A and Iro H. Histopathological comparison of pleomorphic adenomas of the parotid and submandibular gland. *Oral Dis* 2022; 28: 1131-1136.
- [10] Rubini A, Guiban O, Cantisani V and D'Ambrosio F. Multiparametric ultrasound evaluation of parotid gland tumors: B-mode and color Doppler in comparison and in combination with contrast-enhanced ultrasound and elastography. A case report of a misleading diagnosis. *J Ultrasound* 2021; 24: 337-341.
- [11] Kim TY and Lee Y. Contrast-enhanced multi-detector CT examination of parotid gland tumors: determination of the most helpful scanning delay for predicting histologic subtypes. *J Belg Soc Radiol* 2019; 103: 2.
- [12] Park CJ, Kim KW, Lee HJ, Kim MJ and Kim J. Contrast-enhanced CT with knowledge-based iterative model reconstruction for the evaluation of parotid gland tumors: a feasibility study. *Korean J Radiol* 2018; 19: 957-964.
- [13] Roesink JM, Terhaard CH, Moerland MA, van Iersel F and Battermann JJ. CT-based parotid gland location: implications for preservation of parotid function. *Radiother Oncol* 2000; 55: 131-133.
- [14] Bisdas S, Baghi M, Wagenblast J, Knecht R, Thng CH, Koh TS and Vogl TJ. Differentiation of benign and malignant parotid tumors using deconvolution-based perfusion CT imaging: feasibility of the method and initial results. *Eur J Radiol* 2007; 64: 258-265.
- [15] Karaman CZ, Tanyeri A, Ozgur R and Ozturk VS. Parotid gland tumors: comparison of conventional and diffusion-weighted MRI findings with histopathological results. *Dentomaxillofac Radiol* 2021; 50: 20200391.
- [16] Yabuuchi H, Kamitani T, Sagiyama K, Yamasaki Y, Hida T, Matsuura Y, Hino T, Murayama Y, Yasumatsu R and Yamamoto H. Characterization of parotid gland tumors: added value of permeability MR imaging to DWI and DCE-MRI. *Eur Radiol* 2020; 30: 6402-6412.
- [17] Malik A, Devabalan Y, Bernstein J, Awad Z, Gujral D, Partridge S, Madani G, Clarke P, Weir J and Mace A. Malignant salivary gland tumours: single-centre experience of 108 patients. *Clin Otolaryngol* 2021; 46: 1310-1314.
- [18] Tajima Y, Kuroki T, Tsutsumi R, Isomoto I, Uetani M and Kanematsu T. Pancreatic carcinoma coexisting with chronic pancreatitis versus tumor-forming pancreatitis: diagnostic utility of the time-signal intensity curve from dynamic contrast-enhanced MR imaging. *World J Gastroenterol* 2007; 13: 858-865.
- [19] Sone S, Higashihara T, Morimoto S, Ikezoe J, Nakatsukasa M, Arisawa J and Tamaki H. CT of parotid tumors. *AJNR Am J Neuroradiol* 1982; 3: 143-147.
- [20] Dong Y, Lei GW, Wang SW, Zheng SW, Ge Y and Wei FC. Diagnostic value of CT perfusion imaging for parotid neoplasms. *Dentomaxillofac Radiol* 2014; 43: 20130237.
- [21] Mikaszewski B, Markiet K, Smugala A, Stodulski D, Garsta E, Piatkowski J and Szurowska E. Value of dynamic contrast enhanced MRI in differential diagnostics of Warthin tumors and parotid malignancies. *Sci Rep* 2021; 11: 16282.
- [22] Xu Z, Chen M, Zheng S, Chen S, Xiao J, Hu Z, Lu L, Yang Z and Lin D. Differential diagnosis of parotid gland tumours: application of SWI combined with DWI and DCE-MRI. *Eur J Radiol* 2022; 146: 110094.
- [23] Ito K, Muraoka H, Hirahara N, Sawada E, Tokunaga S and Kaneda T. Quantitative assessment of the parotid gland using computed tomography texture analysis to detect parotid sialadenitis. *Oral Surg Oral Med Oral Pathol Oral Radiol* 2022; 133: 574-581.
- [24] Huang N, Chen Y, She D, Xing Z, Chen T and Cao D. Diffusion kurtosis imaging and dynamic contrast-enhanced MRI for the differentiation of parotid gland tumors. *Eur Radiol* 2022; 32: 2748-2759.
- [25] Reerds STH, Marres HAM and Honings J. Response to letter to the editor: regarding the "surgical management of deep lobe parotid tumours with and without involvement of the

Identification of parotid tumors by CT plus MRI

- parapharyngeal space". *Int J Oral Maxillofac Surg* 2022; 51: 1246.
- [26] Yang F, Wu M, Peng Y, Dong X and Ge Y. Do not ignore tuberculosis of the parotid gland when meeting obvious infiltration of neutrophils in a suspicious swelling by FNAC. *Ear Nose Throat J* 2022; 101: NP266-NP269.
- [27] Xiang S, Ren J, Xia Z, Yuan Y and Tao X. Histogram analysis of dynamic contrast-enhanced magnetic resonance imaging in the differential diagnosis of parotid tumors. *BMC Med Imaging* 2021; 21: 194.
- [28] Tretiakow D, Przewozny T and Mikaszewski B. Regarding "accuracy, predictability and prognostic implications of fine-needle aspiration biopsy for parotid gland tumours: a retrospective case series". *Clin Otolaryngol* 2021; 46: 1400-1401.
- [29] Gunduz E, Alcin OF, Kizilay A and Piazza C. Radiomics and deep learning approach to the differential diagnosis of parotid gland tumors. *Curr Opin Otolaryngol Head Neck Surg* 2022; 30: 107-113.
- [30] Abdel Razek AAK, Gadelhak BN, El Zahabey IA, Elrazzak GAEA and Mowafey B. Diffusion-weighted imaging with histogram analysis of the apparent diffusion coefficient maps in the diagnosis of parotid tumours. *Int J Oral Maxillofac Surg* 2022; 51: 166-174.
- [31] Fried DV, Zhu T, Das SK, Shen C, Marks LB, Tan X and Chera BS. Prospective assessment of sparing the parotid ducts via MRI sialography for reducing patient reported xerostomia. *Radiother Oncol* 2022; 172: 42-49.
- [32] Li ZQ, Gao JN, Xu S, Shi Y, Liu X, Li X and Wan J. Multimodal magnetic resonance imaging for the diagnosis of parotid gland malignancies: systematic review and meta-analysis. *Transl Cancer Res* 2022; 11: 2275-2282.
- [33] Huang N, Xiao Z, Chen Y, She D, Guo W, Yang X, Chen Q, Cao D and Chen T. Quantitative dynamic contrast-enhanced MRI and readout segmentation of long variable echo-trains diffusion-weighted imaging in differentiating parotid gland tumors. *Neuroradiology* 2021; 63: 1709-1719.
- [34] Wang P, Yang J and Yu Q. Lymphoepithelial carcinoma of salivary glands: CT and MR imaging findings. *Dentomaxillofac Radiol* 2017; 46: 20170053.